Optimization of the Synthesis of Superparamagnetic Contrast Agents by the Design of Experiments Method

ARTICLE *in* THE JOURNAL OF PHYSICAL CHEMISTRY C · NOVEMBER 2008

Impact Factor: 4.77 · DOI: 10.1021/jp803832k

Optimization of the Synthesis of Superparamagnetic Contrast Agents by the Design of Experiments Method

Delphine Forge,[†] Alain Roch,[†] Sophie Laurent,[†] Horacio Tellez,[†] Yves Gossuin,[‡] Fabian Renaux,[§] Luce Vander Elst,[†] and Robert N. Muller*,[†]

Department of General, Organic and Biomedical Chemistry, NMR and Molecular Imaging Laboratory, University of Mons-Hainaut, 24 Avenue du Champ de Mars, B-7000 Mons, Belgium, Biological Physics Department, University of Mons-Hainaut, 24 Avenue du Champ de Mars, B-7000 Mons, Belgium, and Laboratory of Inorganic and Analytic Chemistry, University of Mons-Hainaut, 24 Avenue du Champ de Mars, B-7000 Mons, Belgium

Received: May 1, 2008; Revised Manuscript Received: October 22, 2008

The synthesis of iron oxide nanoparticles by coprecipitation of ferrous and ferric ions was optimized in aqueous and organic medium. For both syntheses, the influence of different factors on the nanoparticle size was successfully evaluated by the "design of experiments" method. This methodology allows finding in very few runs the optimal experimental conditions to synthesize nanoparticles with a predetermined radius. Aqueous and organic syntheses of magnetite seem to be complementary. The first one leads to smaller magnetite nanoparticles (with radius comprised between 4.9 and 5.7 nm). These particles were stabilized by electrostatic repulsion through a two-step process and needed an additional coating. Conversely, the synthesis in organic medium allows producing, in one step, magnetite nanoparticles embedded within a silica corona. In this protocol, the Ostwald ripening phenomenon seems to play a very important role in the formation of larger magnetite crystals (with radius comprised between 4.8 and 7.7 nm) as well as in the control of their monodispersity. The newly synthesized nanoparticles and the experimental protocol used to produce them have a great potential for future applications in molecular MR imaging, cellular MR imaging, and thermotherapy.

1. Introduction

Superparamagnetic iron oxide nanoparticle suspensions, usually called ferrofluids,[1] are constituted of magnetite (Fe_3O_4) or maghemite (γ-Fe_2O_3) particles with a core radius smaller than 5 nm. Because of such a small core size, each particle can be considered as a single magnetic domain (called Weiss domain).[2] These particles show a superparamagnetic behavior, with a high saturation magnetization. However, the material is completely magnetized at clinical imaging fields. The main application of these superparamagnetic particles is as contrast agents for magnetic resonance imaging (MRI), to enhance the contrast between healthy and pathological tissues.[3,4] Because of their high magnetization, these compounds have an important effect on the water protons transverse relaxation,[5] and are therefore very efficient negative contrast agents.[6] Currently, aqueous dispersions of magnetite nanoparticles embedded in the corona of dextran or one of its derivatives are widely used in clinical MR imaging.[7]

Ferrofluids are not only a very powerful material for medical diagnoses, but they could also be used for therapeutic purposes since tumors cells are highly sensitive to elevated temperatures.[8] When incorporated into a tumor, magnetic particles generate heat under an alternating magnetic field and destroy the tumor without damaging surrounding tissue.[9] This technique is commonly termed rf ablation and has been used primarily to treat liver tumors. For this kind of applications, the knowledge and the control of the chemical and physical characteristics of the nanoparticles[10] are very important. Rosenweg et al.[11] have theoretically proved that the most efficient particles to induce hyperthermia must have a crystal radius of about 7 nm. On the other hand, for Magnetic Resonance Angiography, the crystals should be small and monodisperse to strengthen the T1 effect. For Molecular Imaging, high saturation magnetization are needed for an optimal T2* effect. In cell tracking, the size of the core also regulates the particles uptake by the cells. The optimal formulation will thus vary greatly depending upon the desired indication.

The choice of the synthesis method is thus of paramount importance, since it determines the magnetic nanoparticle's size and shape, as well as its size distribution and surface chemistry. The methods generally used to synthesize magnetic nanoparticles for medical applications include microemulsions,[12] sol−gel synthesis,[13] laser pyrolysis,[14] sonochemical synthesis,[15] and coprecipitation.[16] Among these methods, the coprecipitation of ferrous and ferric salts in an alkaline medium[17,18] is the most commonly used. However, this simple and efficient chemical pathway to obtain magnetite barely allows controlling the particle size at the nanometric scale and the monodispersity. For example, the coprecipitation synthesis of Feridex results in a core radius ranging from 1.5 to 2.5 nm and in a particle size ranging from 20 to 300 nm.[19] Indeed, a large number of experimental factors[20−22] such as [Fe(II)]/[Fe(III)] ratio, iron concentration, pH, temperature, stirring rate, and ionic strength can influence the size of the synthesized iron oxide nanoparticles. Numerous studies[21,23,24] have demonstrated that the mean size increases with the [Fe(II)]/[Fe(III)] ratio. Contrarily, the

* To whom correspondence should be addressed. Phone/Fax: 00-32-65-373520. E-mail: robert.muller@umh.ac.be.
[†] Department of General, Organic and Biomedical Chemistry, NMR and Molecular Imaging Laboratory.
[‡] Biological Physics Department.
[§] Laboratory of Inorganic and Analytic Chemistry.

10.1021/jp803832k CCC: $40.75
Published on Web 11/17/2008

higher the pH is, the smaller the magnetic crystal size and size distribution width will be.

The purpose of this work is to describe the synthetic conditions required to create the optimal core needed based upon the desired application. The influence of the synthesis parameters on the magnetic nanocrystals radius has been investigated in order to develop a reproducible coprecipitation procedure. Two protocols were used: the first one is the conventional coprecipitation in aqueous solution of ferrous and ferric ions in alkaline medium. This method leads to iron oxide particles that need a subsequent coating to ensure their stability at physiological pH. The second method is a one step synthesis of nanoparticles covered in situ with silica. In this original protocol, the coprecipitation is performed in an organic medium that allows working at a higher temperature. The main advantage of this synthesis is the occurrence of the Ostwald ripening,[25] a phenomenon which allows the growth of the bigger particles and hence the synthesis of larger nanocrystals.

In order to optimize the synthesis of magnetite nanoparticles, we used the design of experiments (DoE)[26] method, also known as multivariate analysis. This methodology requires a minimum number of experiments, in which all relevant factors are varied systematically. The analysis of the experimental results allows determining the relationship between the factors affecting a process and the output of that process.[27] It also helps to prove the existence of interactions and synergies between different factors. In our case, in order to optimize the synthesis, the output of the design of experiments is the radius of the nanoparticles as measured by the fitting of the magnetization curves by a Langevin function. This value is compared to the one obtained from the fitting of the nuclear magnetic resonance dispersion (NMRD) profiles.[28]

2. Experimental Methods

2.1. Materials. Ferrous chloride tetrahydrate, ferric chloride hexahydrate and hydrochloric acid (37%) were used to prepare the iron stock solution. Sodium hydroxide was employed as precipitating agent. Diethylene glycol was used as the solvent and silica (silicagel, Merck, grade 60, 70−230 mesh, 60 Å) was employed to ensure the colloidal stability for the synthesis in organic medium. All these reagents were commercially available (Aldrich or Fluka, Bornem, Belgium) and were used without further purification. To ensure the best reproducibility, the syntheses were performed in a reactor (Reactor system 1000 mL, Autoclave Zuid, Antwerp, Belgium) with a perfect control of temperature, reactant flow rate, and stirring rate. The graphs, models, and tables obtained from statistical analyses were produced using Design Expert Software (Version 5.0.3, Stat-ease Inc., Minneapolis, MN, 1997).

2.2. Synthesis of Magnetite Nanoparticles. The basic chemical reaction used in the synthesis of nanoparticles is

$$Fe^{2+} + 2Fe^{3+} + 8OH^- \rightarrow Fe_3O_4 + 4H_2O$$

According to this reaction, an initial $[Fe^{2+}]/[Fe^{3+}]$ molar ratio of 0.5 is needed for the production of Fe_3O_4, but, when the preparation is carried out in the presence of air, Fe^{2+} gets oxidized to Fe^{3+}, leading to the formation of maghemite (γ-Fe_2O_3). To prevent this, nitrogen (N_2) gas was bubbled into the reaction mixture and the reactor was constantly flushed.

2.2.1. Synthesis in Aqueous Medium. In aqueous medium, the following typical experimental procedure[16] was used—a stirred solution of 25 mL of $FeCl_3$ and 6.3 mL of $FeCl_2$ was added to 250 mL of preheated NaOH solution. Vigorous stirring and heating were continued for 10 min. The black gelatinous precipitate that immediately forms was isolated from the solution by magnetic decantation. This was performed by placing the vessel on a permanent magnet ($B_0 = 0.5$ T). This precipitate was then washed five times with a aqueous solution of tetramethylammonium hydroxyde (125 mL, 1 M). Finally, the precipitates were dispersed in deionized water and centrifuged at 10 000 rpm for 15 min to remove the aggregates. This technique results in electrostatically stabilized ferrofluid which requires an additional coating for biomedical applications at pH 7.

TABLE 1: Low, Medium, and High Levels Chosen for the Coprecipitation in Aqueous Medium

	level		
factor	−1	0	+1
$[Fe^{2+}/Fe^{3+}]$ ratio	1	2.5	4
[Fe] (M)	2	5	8
temperature (°C)	30	75	100
pH	9	11	13
reactant flow rate (mL/min)	3.5	36.75	70
stirring rate (rpm)	50	150	250

TABLE 2: Low, medium, and high levels chosen for the coprecipitation in organic medium.

	level		
factor	−1	0	+1
initial temperature (°C)	140	170	200
ripening temperature (°C)	170	190	210
stirring rate (rpm)	50	150	250
volume of the solution (mL)	250	625	1000
initial time (min)	10	65	120
ripening time (h)	1	3.5	6
pH	9	11	14

2.2.2. Synthesis in Organic Medium. The synthesis in organic medium consists of a one-step coprecipitation at high temperature followed by in situ coating with silica. An equimolar mixture (3.3 M with $[Fe^{2+}]/[Fe^{3+}] = 1$) of $FeCl_2$ and $FeCl_3$ in diethyleneglycol solution was heated at a determined temperature. Solid (pellet) NaOH was added in order to prevent the addition of any aqueous media. The silica gel was then added to the mixed solution. This solution was cooled to room temperature. The excess unbound silica was separated by dialysis for 48 h (cutoff membrane: 12−14 000 Spectra/Por VWR, Belgium).

The experimental conditions of these two reactions (molar ratio between ferrous and ferric ions, Fe concentration, temperature, pH of the medium, stirring rate, and reactant flow rate for the reaction in aqueous medium; or volume of the solution, initial and ripening temperature and time, stirring rate, and pH for the coprecipitation in organic medium) were modified for each experiment (Tables 1 and 2).

2.3. Characterization. The magnetite particles were characterized by various techniques. The values of the particle size and the saturation magnetization were first determined by the fitting of experimental magnetometric curves using a Langevin function. The magnetization measurements were performed on a known amount of ferrofluid using a vibrating sample magnetometer (VSM-NUOVO MOLSPIN/ Newcastle Upon Tyne, UK). The fitting of the profiles according to the ad hoc theory gives several parameters as the crystal radius (r) and the specific magnetization (M_S).[29] An additional way to determine the size is the measurement of the proton nuclear magnetic relaxation rate at different magnetic fields. Nuclear magnetic relaxation dispersion (NMRD) profiles were recorded with a field cycling relaxometer (STELAR, Mede, Italy) measuring the longitudinal

relaxation rates (R_1) in a field range extending from 0.24 mT to 0.24 T. The temperature of the samples was adjusted to 37 °C with a precision of 0.1 °C. Additional longitudinal (R_1) and transverse (R_2) relaxation rate measurements at 0.47 and 1.41 T were, respectively, obtained on Minispec PC 120 and MQ 60 spin analyzers (Bruker, Karlsruhe, Germany). The fitting of the NMRD profiles by a theoretical relaxation model[28] allows the determination of r, M_S, and the Néel relaxation time (τ_N).

The size and the shape of the nanocrystals coated with silica were also examined using transmission electron microscopy (TEM) (CM 20, Philips). A small volume of the sample was vaporized on the TEM carbon-coated copper grids in order to avoid artificial aggregation of the particles during the drying of the sample. The mean particle size and the distribution were evaluated by measuring the largest internal dimension of 110 magnetic crystals. The chemical composition of the ferrofluid was characterized using infrared spectroscopy (FT-IR) and Time of flight secondary ion mass spectroscopy (ToF-SIMS) studies. The FT-IR spectrum of the lyophilized sample was recorded between 4000 and 650 cm^{-1} in the transmission mode on a spectrum 100 (Perkin-Elmer, Zaventem, Belgium). ToF-SIMS measurements were made using a ToF-SIMS 4 (Ion Tof, Münster, Germany).

Total iron concentration was determined by proton relaxometry at 20 MHz and 37 °C after microwave digestion (MLS-1200 MEGA, MILESTONE, Analis, Namur, Belgium). Silica concentration was measured by inductively coupled plasma (ICP) (JOBIN YVON JY70+, Longjumeau, France) after microwave digestion.

3. Results and Discussion

3.1. Coprecipitation in Aqueous Medium. Based on our previous results[30,31] and on literature data,[21,23] we investigated the influence of the six following parameters: (i) molar ratio between ferrous and ferric ions, (ii) total iron concentration, (iii) pH of the solution, (iv) stirring rate, (v) temperature, and (vi) reactant flow rate. The high (+1), medium (0), and low (−1) levels for each parameter are reported in Table 1. The design of experiments is composed of two main parts: the screening design (for the identification of key process parameters) and the response surface design (for the modeling of the synthesis). From the screening experiments, it was determined that (i) $[Fe^{2+}]/[Fe^{3+}]$ ratio, (ii) iron concentration, (iii) temperature, and (iv) stirring rate are important factors controlling the size of nanoparticles (results not shown).[32]

The influence of these factors on the nanoparticle size was thus evaluated by the response surface design in order to optimize and model the synthesis of nanoparticles in aqueous medium. The total number of runs needed to build up this design was 29, as proposed by the Box-Behnken design.[33] Five replicates of the center points were run in order to evaluate the standard deviation associated with the model. The nanoparticles obtained with this type of synthesis are characterized by a range of radii extending from 4.9 to 5.7 nm (Figure 1). The standard deviation of this model is estimated at 0.085 nm.

The formation of magnetite crystals by the coprecipitation method is a two-stage process.[34] The first step is the nucleation, i.e. the formation of crystal embryos when the concentration of the species is above the supersaturation conditions, while the second step is the slow growth of the nuclei by diffusion of the solutes to the crystal surface. During the growth phase, the concentration of free reactant should be adjusted between the supersaturation and the solubility concentration in order to produce monodisperse iron oxide nanoparticles. For iron oxides, this condition is difficult to obtain because the values of the supersaturation and solubility are very close. In these conditions, the growth of the crystals and the formation of new nuclei occur at the same time, so the produced nanoparticles are not systematically monodisperse.

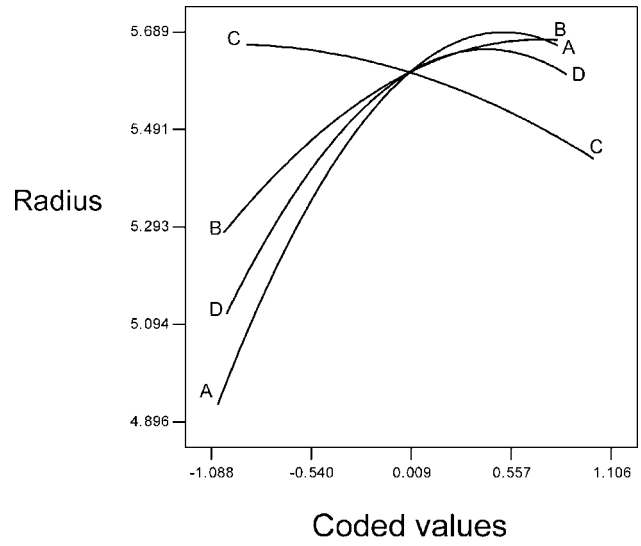

Figure 1. Factor plot (A, $[Fe^{2+}]/[Fe^{3+}]$ ratio; B, iron concentration; C, stirring rate; D, temperature) for the synthesis in aqueous medium.

Figure 1 shows the estimated radius of nanoparticles as a function of each experimental parameter. In the plot, the factor of interest is varied from its low level (−1) to its high level (+1), while all other factors are held constant at their central values (0). In our experimental setup, the most important factor is the $[Fe^{2+}]/[Fe^{3+}]$ ratio (curve A). As it increases from −1 to +1 in coded values, the particle size increases because the supersaturation level decreases. The growth of the nucleated crystals is favored allowing the formation of larger particles, in agreement with literature data.[20,21] Similarly, as the iron concentration (curve B) and temperature (curve D) increase from −1 to +1 in coded values, the nanoparticle radius increases. The growth process of nucleated crystallites[35] helps to understand these results: in a diffusion limited growth process, the concentration gradients and the temperature are key factors since the solute is to be supplied to the depleted region near the particle surface via mass transfer from the bulk solution. Conversely, as the stirring rate (curve C) increases from −1 to +1 in coded values, the size of particles decreases. According to Mullin,[36] an increase of stirring rate induces a nucleation mechanism to the detriment of crystalline growth. Therefore, a high stirring rate leads to smaller crystals. According to the literature, the mean size of the crystals greatly decreases on increasing pH and ionic strength.[28,37] Indeed, a change in the surface's electrical charge due to pH leads to a change in the chemical composition of the interface, inducing a decrease of the interfacial tension γ and of the free enthalpy of particles allowing the increase of surface to volume ratio. In our case, whatever the range of the pH (9→13), the surface of the particles is highly charged and therefore does not influence the radius of the magnetite. The particle size is also independent of the reactant flow rate in the coprecipitation medium. This indicates that the particles formed at the beginning of the precipitation do not serve as secondary nucleation sites. For the three parameters A, B, and D, the curves seem to pass by a maximum or to tend toward a plateau.

The two critical 3D surface plots (Figure 2) show that the maximum radius obtained with this protocol is 5.7 nm when

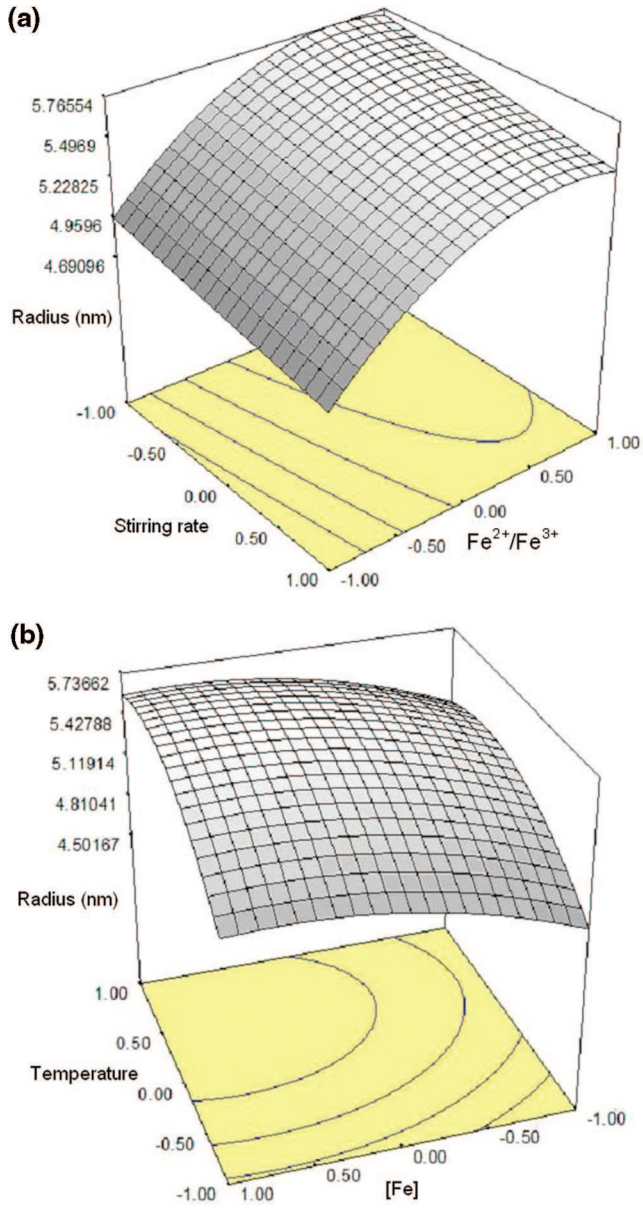

Figure 2. (a) 3D surface response plot for the effects of stirring rate and $[Fe^{2+}]/[Fe^{3+}]$ ratio on the radius of nanoparticles (iron concentration, 8 M; temperature, 100 °C) and (b) 3D surface response plot for the effects of iron concentration and temperature on the radius of nanoparticles ($[Fe^{2+}]/[Fe^{3+}]$ ratio, 4; stirring rate, 50 t/min) for the synthesis in aqueous medium.

working under ideal conditions (high level for $[Fe^{2+}]/[Fe^{3+}]$ ratio, for iron concentration, and for temperature and low level for stirring rate). So, if particles with a larger size are wanted, the experimental protocol must be changed.

3.2. Coprecipitation in Organic Medium. As the Massart synthesis does not allow reaching radii of about 7 nm, which could be interesting for some biomedical applications such as hyperthermia,[8] we have developed a new synthesis that makes it possible to obtain larger nanoparticles of magnetite. A high temperature synthesis in diethylene glycol (DEG) was chosen. Caruntu et al.[38] found that DEG, which can be used as solvent for the synthesis, can act as well as a capping agent of the particles. The authors have shown that the formation of a chelate between iron and the DEG molecules ensures a better control of the hydroxylation, which initiates the iron oxide formation process.

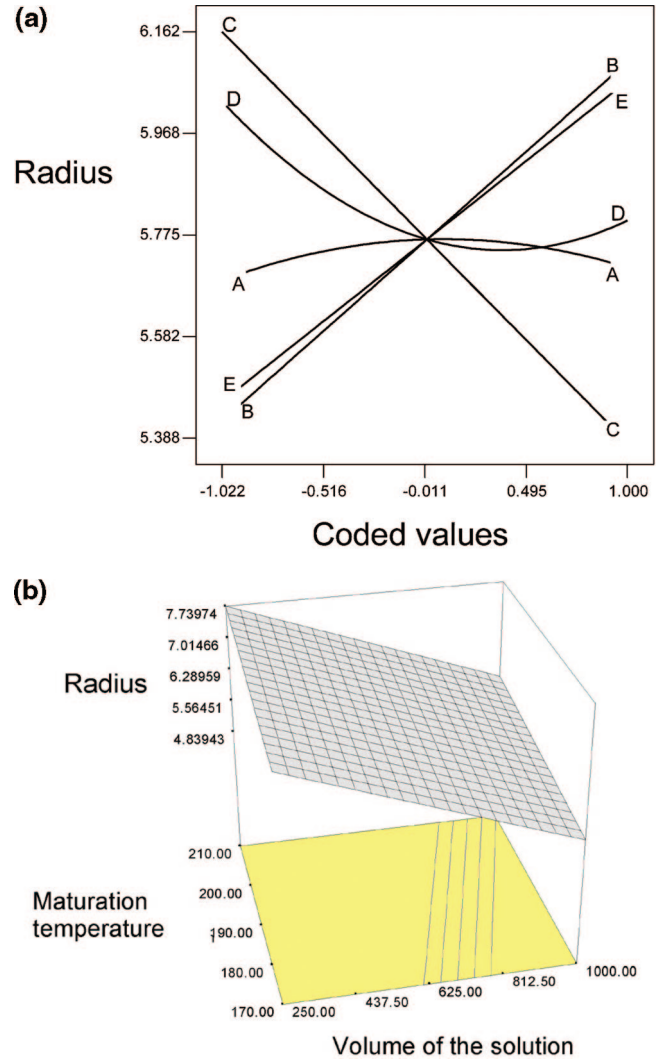

Figure 3. (a) Factor plot (A, initial temperature; B, maturation temperature; C, volume of the solution; D, initial time; E, maturation time) and (b) 3D surface response plot for the effects of maturation temperature and volume of the solution on the radius of nanoparticles (initial temperature, 200 °C; initial time, 120 min; maturation time, 6 h) for the synthesis in organic medium.

Unlike the synthesis discussed above, this protocol includes the coating of the nanocrystals by a slow deposition of silica. This coating prevents particle aggregation in liquids and thus improves their colloïdal stability. Another advantage of a silica-enriched surface is the presence of surface silanol groups. These groups can easily react with various coupling agents to covalently attach specific ligands on the surface of the magnetic particles such as those needed to vectorize the magnetic moeity to a biological target.[39−41] Silica was chosen in spite of its questionable biocompatibility, because it was intensively used in the literature. However, some groups have reported the formation of large iron cores using more biocompatible approaches.[42]

Preliminary experiments carried out to develop this protocol show the potential influence of seven factors on the size of the nanoparticles: (i) the stirring rate, (ii) the volume of the solution, (iii) the pH, (iv) the initial and (v) the maturation temperatures, and (vi) the initial and (vii) the maturation times. The high, medium, and low levels for each factor are reported in Table 2. The initial and maturation temperatures are the temperatures of the solution before and after, respectively, the addition of NaOH. Similarly, the initial time is the time elapsed between

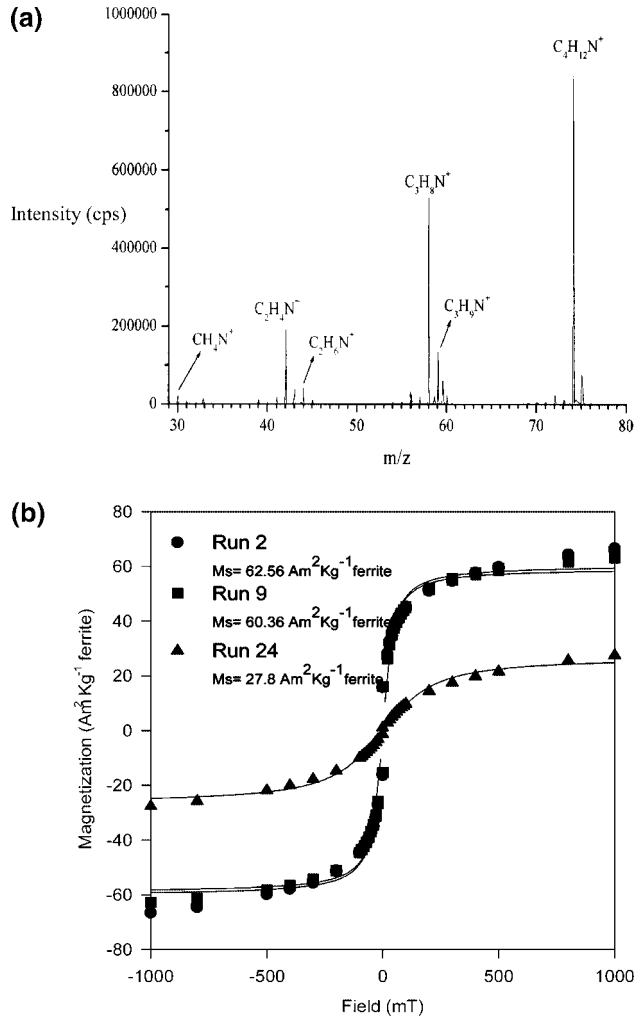

Figure 4. (a) ToF-SIMS spectrum (positive mode) of an alkaline ferrofluid and (b) comparison of the magnetometric curves of three batches synthesized in an aqueous medium and characterized by different $[Fe^{2+}]/[Fe^{3+}]$ ratios (run 2, $[Fe^{2+}]/[Fe^{3+}] = 4$; run 9, $[Fe^{2+}]/[Fe^{3+}] = 2.5$; and run 24, $[Fe^{2+}]/[Fe^{3+}] = 1$).

the setting of the desired temperature and the addition of NaOH, while the maturation time is the time elapsed between the addition of NaOH and the addition of silica.

Five important factors were identified during the screening step: (i) the volume of the solution, (ii) the ripening time, (iii) the ripening temperature, (iv) the initial time, and (v) the initial temperature (results not shown).[43] The nanoparticle size for the 46 statistically designed combinations suggested by the response surface design for the five variables was experimentally determined. Six replicates of the center points were run in order to evaluate the standard deviation associated with the model which was estimated at 0.12 nm. The minimum and maximum radii of nanoparticles obtained were 5.4 and 6.2 nm, respectively (Figure 3a). From this figure, we can see an increase of the nanoparticle size with increasing temperature (curve B) and time of maturation (curve E). The Ostwald ripening[25] seems to have an important effect on the tailoring of iron oxide nanoparticles. In fact, the higher surface energy of the smaller nanoparticles promotes their dissolution, while the solute is redeposited on the larger nanoparticles. Consequently, the average size of nanomagnets increases with time, with a compensating decrease in the number of nanoparticles. A higher solution temperature also favors Ostwald ripening and leads to larger nanoparticles. The driving force of the process is the interfacial tension γ, causing a decrease of the particle surface area, A, in order to bring a negative contribution to the free enthalpy of the transformation ($\Delta G = \gamma \Delta A$).[37] It also can be observed that the volume of the solution (curve C) has an effect on the size of the nanoparticles. As this factor increases from -1 to $+1$ in coded values, the radius of nanomagnets decreases. This shows that the volume of the solution significantly contributes to reducing the size of nanoparticles. In fact, depending on the volume of the solution, the rate of dissolution and homogenization of NaOH is different and therefore the resulting gradient of base concentration seems to perturb the mechanisms of nucleation and of crystal growth.

A 3D contour plot (Figure 3b) shows the effect of maturation temperature and volume of the solution when the other factors are kept at their optimal values. From this plot, it may be deduced that a size of 7.7 nm can be achieved with this protocol when working with the maximum maturation temperature and the smallest solution volume. This hypothesis was confirmed experimentally (the radius obtained was equal to 7.6 nm). It should be possible to increase this optimum by extrapolating the field of the study, but here we are limited by our

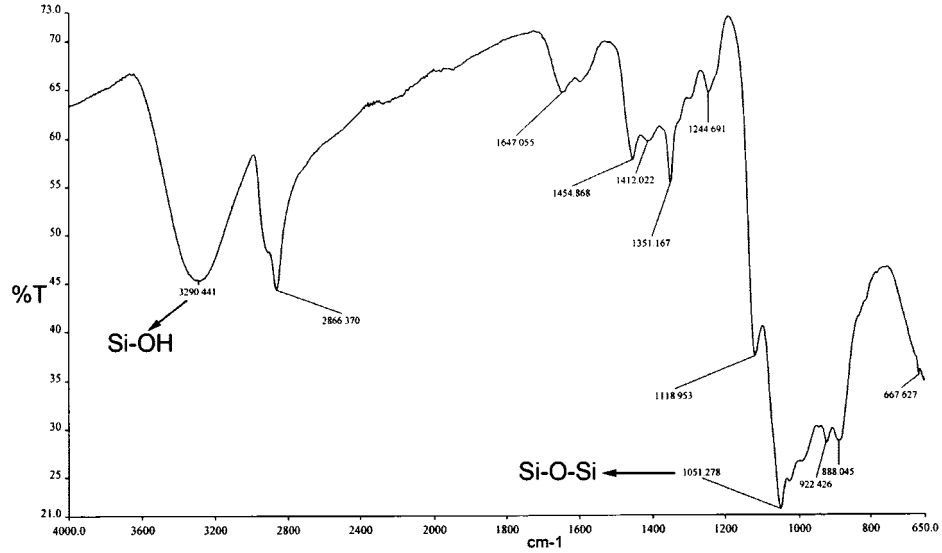

Figure 5. FTIR spectrum of superparamagnetic nanoparticles coated with silica.

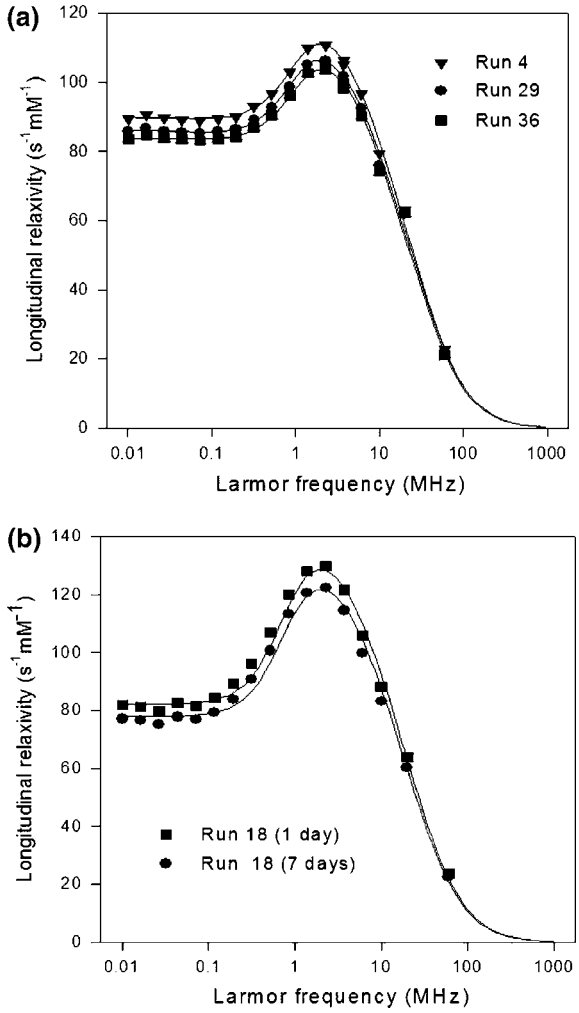

Figure 6. Comparison of (a) the NMRD profiles of three of the six replicates and (b) the relaxometric curves of experiment 18 recorded 1 and 7 days after the synthesis in organic medium.

experimental setup to a temperature not higher than 210 °C and a minimum volume of 250 mL.

3.3. Characterization of Iron Oxides. ***3.3.1. Coprecipitation in Aqueous Medium.*** Magnetite's isoelectric point is observed at a pH of 6.8.[44] Around this point, called the point of zero charge (PZC), the surface charge density (Σ) is very weak. Therefore, the interparticle electrostatic repulsions are smaller than the van der Waals attractive and magnetic forces causing the flocculation of the ferrofluid. In order to prevent particle aggregation due to the attractive van der Waals or magnetic dipole−dipole interactions, a repulsive force between particles must be created by means of electrostatic or sterical protection. The electrostatic field developing around magnetite particles under acidic and alkaline conditions far from the PZC's pH can prevent the aggregation of particles with similar charges due to the repulsion of their overlapping electric double layers. However, the colloidal dispersion stability of magnetite via electrostatic stabilization is possible only when the counterion is a weak polarizing species such as NO_3^- in acidic medium or $N(CH_3)_4^+$ in alkaline medium.[16,44] These counterions can be identified by time-of-flight secondary ion mass spectrometry (ToF-SIMS). Indeed, as figure 4a shows, a series of peaks corresponding to the fragments of TMAOH ($N(CH_3)_4^+$ m/z = 74) are observed, indicating that the stability of the magnetite can be achieved.

Figure 4b shows the magnetization curves of three alkaline ferrofluids obtained with a different $[Fe^{2+}]/[Fe^{3+}]$ ratio. These magnetic measurements indicate a superparamagnetic behavior at room temperature for all samples, with no hysteresis and a perfect Langevin behavior. As observed above, the nanomagnet properties can be essentially controlled by the $[Fe^{2+}]/[Fe^{3+}]$ ratio. Indeed, the saturation magnetization and therefore the nanomagnet radius both increase with this ratio. However, the saturation magnetization value of run 24 ($[Fe^{2+}]/[Fe^{3+}]$ = 1, [Fe] = 2 M, stirring rate = 150 rpm, temperature = 75 °C) is lower than the reported data for bulk magnetite (70−80 A·m^2/kg).[1] This can be explained by the larger surface/volume ratio and the subsequent surface spin effects, which can modify the saturation magnetization of a magnetic material usually by lowering their magnetization.[45] As the particle radius increases [run 2 ($[Fe^{2+}]/[Fe^{3+}]$ = 4) and 9 ($[Fe^{2+}]/[Fe^{3+}]$ = 2.5)], the surface/volume ratio becomes smaller and, therefore, the saturation magnetization gets close to the bulk magnetite value. With a ratio equal to 2, the samples have similar saturation magnetization because the organized particle spins become the dominant part of the magnetic material.

3.3.2. Coprecipitation in Organic Medium. In this synthesis, a silica coating is formed around iron oxide nanoparticles and thus the stabilization of the nanomagnets is due to sterical and to electrostatic repulsions because of the presence of negative charges on the iron oxide surface. The presence of silica at the surface of magnetite crystals was determined by ToF-SIMS by finding a $Si_2O_5^-/FeO^-$ ratio equal to 3.15 and by infrared spectroscopy (FT-IR) analysis (Figure 5). The wide band around 3290 cm^{-1} is characteristic of hydroxyl groups of water adsorbed by H-bridging on surface silanol groups. The spectrum also shows a strong band around 1051

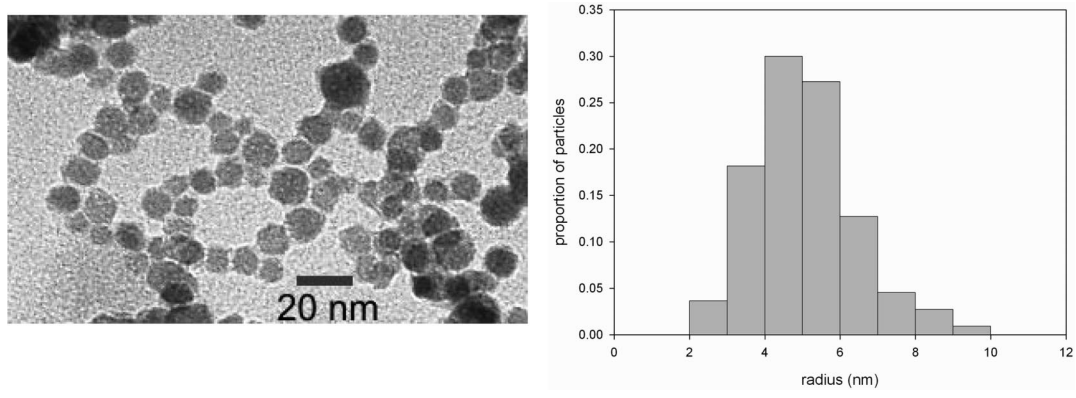

Figure 7. TEM image of nanoparticles coated by silica synthesized in organic medium and their size distribution.

cm^{-1} originating from siloxane bonds (Si−O−Si). According to the experimental conditions (SiO_2/Fe_3O_4 ratio, temperature, pH, etc.), the silica oligomers can condensate with the superficial Fe-OH groups on the iron oxide nanoparticles to form siloxanes bonds. These bonds will make it possible to reinforce the silica coating and prevent aggregation. To estimate the thickness of the layer of silica around the particles, the silica concentration obtained by inductively coupled plasma (ICP) was compared to the surface/volume ratio (estimated theoretically) of a nanoparticle. According to this comparison, a bilayer of silica (10 Å) is supposed to form at the surface of the particles. The capping role of diethylene glycol was also proved by FT-IR. Indeed, the bands at 2866 (C−H), 1118 (C−O), 1454, and 1351 cm^{-1} could be assigned to the diethylene glycol by comparison with a reference spectrum.

The analysis of the NMRD profiles (Figure 6a) of the different particles was used as a complementary technique to characterize the iron oxide crystal. The remarkable similarity of the profiles at low field demonstrates the perfect reproducibility between different syntheses. The mean size and the mean specific magnetization for the replica measured by relaxometry are, respectively, $r_{\text{relaxo}} = 6.8$ nm and $M_{\text{s relaxo}} = 59.3$ $A \cdot m^2/kg$. The corresponding values obtained by magnetometry are $r_{\text{magneto}} = 5.8$ nm and $M_{\text{s magneto}} = 74.3$ $A \cdot m^2/kg$. As expected,[46] the radius evaluated using magnetometry is smaller than the one obtained by relaxometry. This difference can indeed be explained by a distribution of the crystal sizes which influences, with different weighing, the mean size obtained by various methods. This size distribution is also responsible for the lower relaxometric specific magnetization as compared to the magnetometric one.

Although their very high sensitivity to any chemical or physical modification make the NMRD profiles very well suited to control the reproducibility of the nanomagnet synthesis, they can be also used to control the stabilization efficiency. Two NMRD profiles (Figure 6b) recorded on the same sample one day and one week after the synthesis were compared in order to evaluate the degree of the stabilization by silica. As proved by the similarity of the curves, the values of SiO_2/Fe_3O_4 used currently are sufficient to reach an optimal stability.

The size distribution of the spherical iron oxide core was evaluated by transmission electron microscopy (Figure 7). The average radius is estimated at 5.1 nm. This radius seems to coincide with the values obtained by magnetometry ($r = 5.8$ nm) and relaxometry ($r = 6.4$ nm); however, some polydispersity is observed. A size sorting procedure is in progress in order to reduce the size dispersion in the solution.

4. Conclusions

Magnetite nanoparticles were synthesized via a coprecipitation method of ferrous and ferric ions in aqueous and organic medium, using the DoE methodology. DoE is a powerful tool allowing the determination of the most important parameters and the modeling of these syntheses. The optimal experimental conditions for obtaining magnetite crystals of a predetermined size with a high precision were established.

In organic medium, the Ostwald ripening seems to be the most important factor for controlling the size and the monodispersity of the magnetite particles. This one-step synthesis allows obtaining a larger crystal radius, comprised between 4.8 and 7.7 nm. Moreover, a bilayer of silica is formed around the particle surface and ensures the stabilization of the nanoparticles.

Acknowledgment. The authors thank Mrs. Patricia de Francisco for her help in preparing the manuscript. The authors also thank Materia Nova for transmission electron microscopy (TEM) and for the time-of-flight secondary ion mass spectroscopy (ToF-SIMS) studies. D.F. is grateful to the FRIA for financial support. Support and sponsorship of the COST Action D38, EMIL NoE program, NOMADE program of the Walloon Region, ARC program of the French Community of Belgium are kindly acknowledged.

Supporting Information Available: A description of the design of experiments methodology is presented in the Supporting Information section. This material is available free of charge via the Internet at http://pubs.acs.org.

References and Notes

(1) Schwertmann, U.; Cornell, R. M. *The Iron Oxide*; VCH: Weinheim, Cambridge, 1991.
(2) Chatterjee, J.; Haik, T.; Chen, C. *J. Magn. Magn. Mater.* **2003**, *257*, 113.
(3) Weissleder, R.; Bogdanov, A.; Neuwelt, E. A.; Papisov, M. *Adv. Drug. Deliver. Rev.* **1995**, *16*, 321.
(4) Muller, R. N.; Vander Elst, L.; Roch, A.; Peters, J. A.; Csajbok, E.; Gillis, P.; Gossuin, Y. *Adv. Inorg. Mater.* **2005**, *57*, 239.
(5) Mendonca Dias, M. H.; Lauterbur, P. C. *Magn. Reson. Med.* **1986**, *3*, 328.
(6) Arnold, P.; Ward, J.; Wilson, D.; Guthie, J. A.; Robinson, P. J. *J. Magn. Reson. Imaging* **2003**, *21*, 695.
(7) Lind, K.; Kresse, M.; Debus, N. P.; Muller, R. H. *J. Drug Target* **2002**, *10*, 221.
(8) Jordan, A.; Scholz, R.; Wust, P.; Fähling, H.; Felix, R. *J. Magn. Magn. Mater.* **1999**, *201*, 413.
(9) Matsuki, H.; Satoh, T.; Murakami, K.; Hoshino, T.; Yanada, T.; Kikushi, S. *IEEE Trans. Magn.* **1990**, *26*, 1551.
(10) Tarjaj, P.; Morales, M. P.; Veintemillas-Verdaguer, S.; Gonzales-Carreño, T.; Serna, C. *J. Magn. Magn. Mater.* **2005**, *290*, 28.
(11) Rosensweig, R. E. *J. Magn. Magn. Mater.* **2002**, *252*, 370.
(12) Deng, Y.; Wang, L.; Yang, W.; Fu, S.; Elaissari, A. *J. Magn. Magn. Mater.* **2003**, *257*, 69.
(13) Albornoz, C.; Jacobo, S. E. *J. Magn. Magn. Mater.* **2006**, *305*, 12.
(14) Bomati-Miguel, O.; Morales, M. P.; Tartaj, P.; Ruiz-Cabello, J.; Bonville, P.; Santos, M.; Zhao, X.; Veintemillas-Verdaguer, S. *Biomaterials* **2005**, *26*, 5695.
(15) Kim, E. H.; Lee, H. S.; Kwak, B. K.; Kim, B. K. *J. Magn. Magn. Mater.* **2005**, *289*, 328.
(16) Massart, R. *IEEE Trans. Magn.* **1981**, *17*, 1247.
(17) Jiang, W.; Yang, H. C.; Yang, S. Y.; Horng, H. E.; Hung, J. C.; Chen, Y. C.; Hong, C. Y. *J. Magn. Magn. Mater.* **2004**, *283*, 210.
(18) Bee, A.; Massart, R.; Neveu, S. *J. Magn. Magn. Mater.* **1995**, *149*, 6.
(19) Laurent, S.; Forge, D.; Port, M.; Roch, A.; Robic, C.; Vander Elst, L.; Muller, R. N. *Chem. Rev.* **2008**, *108*, 2064.
(20) Massart, R.; Cabuil, V. *J. Chim. Phys.* **1987**, *84*, 967.
(21) Babes, L.; Denizot, B.; Tanguy, G.; Le Jeune, J.-J.; Jallet, P. *J. Colloid Interface Sci.* **1999**, *212*, 474.
(22) Jolivet, J. P.; Belleville, P.; Tronc, E.; Livage, J. *Clays Clay Miner.* **1992**, *40*, 531.
(23) Vayssières, L.; Chanéac, C.; Tronc, E.; Jolivet, J.-P. *J. Colloid Interface Sci.* **1998**, *205*, 205.
(24) Jolivet, J. P.; Tronc, E.; Chanéac, C. C. R. *Chimie* **2002**, *5*, 659.
(25) Sugimoto, T. *Chem. Eng. Technol.* **2003**, *26*, 3.
(26) Goupy, J. Introduction aux plans d'expériences, Paris: Dunod 2005.
(27) Capetti, N.; Donnarumma, A.; Naddeo, A.; Russo, L. *J. Mater. Process. Technol.* **2006**, *175*, 77.
(28) Roch, A.; Muller, R. N.; Gillis, P. *J. Chem. Phys.* **1999**, *110*, 5403.
(29) Rosensweig, R. E.; *Cambridge Monographs on Mechanics and Applied Mathematics*; Cambridge University Press: New York, 1985.
(30) Ouakssim, A.; Fastrez, S.; Roch, A.; Laurent, S.; Gossuin, Y.; Pierart, C.; Vander Elst, L.; Muller, R. N. *J. Magn. Magn. Mater.* **2004**, *272*, e1711.
(31) Laurent, S.; Nicotra, C.; Gossuin, Y.; Roch, A.; Ouakssim, A.; Vander Elst, L.; Cornant, M.; Soleil, P.; Muller, R. N. *Phys. Status Solidi* **2004**, *12*, 3644.
(32) Forge, D.; Tellez, H.; Laurent, S.; Gossuin, Y.; Roch, A.; Vander Elst, L.; Muller, R. N. "Application of the Experiment Design Method to the Synthesis of Superparamagnetic Colloïds", presented at Symposium on Magnetic Separation and Nanomagnetics, Karlsruhe, Germany, October 4−5, 2006.

(33) Goupy, J. Plans d'expériences pour surfaces de réponse, Paris: Dunod1999.

(34) LaMer, V. K.; Dinegar, R. H. *J. Am. Chem. Soc.* **1950**, *72*, 4847.

(35) Cushing, B. L.; Kolesnichenko, V. L.; O'Connor, C. J. *Chem. Rev.* **2004**, *104*, 3893.

(36) Mullin, J. W. *Crystallization*; Butterworth-Heinemann: Oxford, 1993.

(37) Jolivet, J. P.; Tronc, E.; Chanéac, C. *Eur. Phys. J.* **2000**, *10*, 167.

(38) Caruntu, D.; Remond, Y.; Chou, N. H.; Jun, M. J.; Caruntu, G.; He, J.; Goloverda, G.; O'Connor, C.; Lolesnichenko, V. *Inorg. Chem.* **2002**, *41*, 6137.

(39) del Campo, A.; Sen, T.; Lellouche, J.-P.; Bruce, I. J. *J. Magn. Magn. Mater.* **2005**, *293*, 33.

(40) Mornet, S.; Portier, J.; Duguet, E. *J. Magn. Magn. Mater.* **2005**, *293*, 127.

(41) Boutry, S.; Laurent, S.; Vander Elst, L.; Muller, R. N. *Contrast Med. Mol. Imaging* **2006**, *1*, 15.

(42) Lee, H. Y.; Lee, S.-H.; Xu, C.; Xie, J.; Lee, J. H.; Wu, B.; Koh, A.; Wang, X.; Nishimura, D. G.; Biswal, S.; Sun, S.; Cho, S. H.; Chen, X. *Nanotechnology* **2008**, *19*, 1.

(43) Forge, D.; Laurent, S.; Roch, A.; Gossuin, Y.; Renaux, F.; Vander Elst, L.; Muller, R. N. "Synthesis and characterization of magnetite nanoparticles stabilized by silica", presented at the Cost Chemistry D38 meeting, Eindhoven, Netherlands, May 3−5, 2007.

(44) Bacri, J.-C.; Perzynski, R.; Salin, D. *J. Magn. Magn. Mater.* **1990**, *85*, 27.

(45) Roca, A. G.; Morales, M. P.; O'Grady, K.; Serna, C. J. *Nanotechnology* **2006**, *17*, 2783.

(46) Roch, A.; Lucet, I.; Pouliquen, D.; Anseau, M.; Muller, R. N."Characterisation of superparamagnetic colloids: significance of their crystal size measurements" presented at 4th Annual Meeting of the Society for Magnetic Resonance in Medicine. New York, April 27-May 3, 1996.

JP803832K